

## ARTICLE

# New polyester biodegradable scaffolds for chondrocyte culturing: Preparation, properties, and biological activity

Agnieszka Gadomska-Gajadhur<sup>1</sup>  | Aleksandra Kruk<sup>1,2</sup> | Judyta Dulnik<sup>3</sup> | Andrzej Chwojnowski<sup>4</sup>

<sup>1</sup>Faculty of Chemistry, Warsaw University of Technology, Warsaw, Poland

<sup>2</sup>Faculty of Pharmacy, Medical University of Warsaw, Warsaw, Poland

<sup>3</sup>Institute of Fundamental Technological Research PAS, Warsaw, Poland

<sup>4</sup>Nalęcz Institute of Biocybernetics and Biomedical Engineering PAS, Warsaw, Poland

## Correspondence

Agnieszka Gadomska-Gajadhur, Faculty of Chemistry, Warsaw University of Technology, Noakowskiego 3, 00-664 Warsaw, Poland.  
Email: agnieszka.gajadhur@pw.edu.pl

## Funding information

Politechnika Warszawska

## Abstract

An innovative modification of the wet inversion phase method, consisting in the use of a polymer nano-nonwoven as a nonclassic pore precursor. Mechanical properties of the obtained scaffolds were determined, their hydrophilic properties (serum absorbability) were tested, and the content of residues of materials used in the scaffold preparation was determined. Nontoxicity of the developed scaffolds toward T lymphocyte cells was proved. Cultures of primary chondrocytes were obtained successfully. It was proved that an addition of a polymer nano-nonwoven changes the properties of the scaffolds favorably in respect of their subsequent application in tissue engineering.

## KEYWORDS

cartilage regeneration, chondrocytes, nano-nonwoven, polyvinylpyrrolidone, T lymphocytes

## 1 | INTRODUCTION

Treatment of joint cartilage lesions poses a big challenge for contemporary medicine,<sup>1</sup> because the cartilage is composed of a tissue belonging to those hardest to regenerate.<sup>2</sup> This is caused by the fact that chondrocytes, or cartilage tissue cells, require the presence of a three-dimensional (3D) framework for their growth.<sup>3</sup> In healthy tissue, this framework is constituted by the extracellular matrix (ECM), which does not occur in damaged tissue.<sup>4,5</sup> Cellular scaffolds may be a solution to this problem.<sup>6</sup> There are porous volumetric structures, aimed for temporary replacement of the ECM in a damaged tissue.<sup>7</sup> Optionally, the scaffolds may be composed of biodegradable polymers, having a great advantage as there is no

need to remove the implant when the treatment is complete.<sup>8,9</sup>

The extracellular matrix is a very important element of tissues.<sup>10</sup> It consists of a structured form (collagen, elastin, and reticular fibrils), an amorphous form (a mixture of polysaccharides, proteins, and proteoglycans), and extracellular fluid (a solution of chemical elements, ions, and micromolecular compounds).<sup>11,12</sup> In tissue, the ECM plays a variety of important roles, it constitutes the spot of cell fixation and the physical tissue framework, as well as imparts mechanical strength and elasticity to the tissue.<sup>12–14</sup> When a tissue is damaged, the extracellular matrix is destroyed too. Therefore, its temporary replacement is necessary.<sup>15</sup>

Tissue damages pose a very big problem for both physicians and patients because the damage hinders or prevents movement and cause a lot of pain.<sup>16</sup> At present, cartilage treatment is carried out by microfractures,<sup>17</sup> autologous cartilage implantation (ACI),<sup>18</sup> and cartilage

**Abbreviations:** iPrOH, isopropanol; PCL, poly-ε-caprolactone; PCLA, poly(L-lactide-co-ε-caprolactone); PEG, poly(ethylene glycol); PLLA, poly-L-lactide; PVP, polyvinylpyrrolidone; SEM, scanning electron microscopy.

implantation.<sup>19</sup> The microfractures method consists of drilling microholes in the subchondral bone to induce the release of stem cells, which will transform into chondrocytes. In spite of its simplicity, the method has a disadvantage consisting in the formation of mainly the undesirable fibrocartilage.<sup>20</sup>

In the two-stage ACI method, chondrocytes are collected from the unloaded part of the cartilage and implanted into the damaged spot.<sup>21</sup> This procedure is lengthy and, as the former, poses the risk of formation of fibrocartilage and tissue hypertrophy.<sup>22,23</sup> Cartilage transplantation is limited by the number of donors and the possibility of transplant rejection.<sup>24</sup> Due to all of the above limitations, a search for methods eliminating these problems commenced, thus reaching for solutions of tissue engineering, namely application of 3D scaffolds.<sup>25,26</sup>

The goal of the study was to obtain scaffolds meeting the requirements necessary for culturing chondrocytes, or for the regeneration of joint cartilage. The key features required for this application are:

- adequate size of pores present in the scaffold fracture (20  $\mu\text{m}$  at minimum), as well as their open character and presence of perforation in their side walls;
- the high porosity of at least one of the scaffold surfaces and presence of pores having an adequate size (20  $\mu\text{m}$  at minimum);
- biodegradability of the scaffolds;
- good mechanical strength (Young modulus at strain  $>10$  MPa),
- adequate hydrophilicity of the scaffolds;
- biocompatibility of the scaffolds (number of alive cells after 24 hr of contactless test  $>70\%$ );
- possibility of culturing chondrocytes on the surface of the scaffold and inside it.

Adequate pore size creates the possibility for the cells to position inside the pores, and it amounts to 20  $\mu\text{m}$  at minimum for chondrocytes.<sup>27</sup> Open and perforated pores ensure intercellular communication and migration of metabolites and nutrients.<sup>5</sup>

Additionally, the pores should be larger than minimum cell size,<sup>28</sup> because the forming tissue must have space for the construction of its structure.<sup>29</sup> However, the pores may not reach too large a size (150–200  $\mu\text{m}$ ), as it could weaken the scaffold structure.<sup>30</sup> The hierarchic structure of the pores determines the properties of the scaffold itself,<sup>31</sup> the possibility of cell and nutrient migration,<sup>32</sup> and cellular adhesion.<sup>33,34</sup>

Adequate porosity of at least one of the scaffold surfaces and presence of pores on it having dimensions adequate for cell (20  $\mu\text{m}$  at minimum)<sup>35</sup> are the

requirements for the cells to be able to penetrate the interior of the scaffold.<sup>36–39</sup>

Even distribution of the pores is required for the formation of a compact tissue.<sup>40</sup> Open and perforated pores ensure intercellular communication and migration of metabolites and nutrients.<sup>41</sup>

Biodegradability of the scaffolds is an optional feature. Due to a gradual, controlled degradation of the material during treatment, it enhances the patient's comfort, because the scaffold used does not remain in their organism.<sup>42,43</sup> Using biodegradable materials, adequate time of their degradation should be chosen, both for the impact of physiological pH<sup>44</sup> when the chondrocytes are cultured,<sup>45</sup> and under storage conditions.<sup>46</sup> The materials cannot lose their structural and mechanical properties too fast.<sup>47</sup>

Adequate mechanical strength of the scaffold is necessary for it to perform the correct function in a joint, and it must be close to that of natural tissue.<sup>48</sup> Young modulus at the strain of the cartilage amount to approximately 10 MPa.<sup>49</sup>

Because of hydrophilic conditions in the tissue, adequate hydrophilicity of the scaffolds is also required.<sup>50</sup> Commonly used synthetic polyesters are hydrophobic,<sup>51</sup> therefore, their modification by application of proper additives in the form of pore precursors is necessary.<sup>52</sup>

Biocompatibility is an essential feature of the scaffolds as medical products and means a lack of toxicity toward cells occurring in organisms.<sup>53,54</sup>

Specific cell types have their preferences in regard to growth—they require specific surface properties enabling their growth.<sup>55</sup> In principle, the possibility of given cells on the examined material should be tested experimentally.<sup>56</sup> In the case of scaffolds replacing cartilaginous tissue, the materials must provide conditions proper for chondrocyte culturing.<sup>57</sup>

Considering all of the above features, it should be noted that scaffold designing is a challenging task.<sup>58</sup> The difficulty results from the necessity of a complex combination of all these features.<sup>59,60</sup>

## 2 | MATERIALS AND METHODS

Poly-L-lactide (PLLA),  $M_n$  86,000 g/mol (Nature Works NW 2003D), poly- $\epsilon$ -caprolactone (PCL),  $M_n$  80,000 g/mol (Sigma Aldrich), and poly(L-lactide-co- $\epsilon$ -caprolactone) (PCLA), prepared in-house, were used to prepare membranes. Poly(vinylpyrrolidone) (PVP),  $M_n$  10,000 g/mol (Sigma Aldrich), poly(ethylene glycol) (PEG)  $M_n$  10 kg/mol (Sigma Aldrich), and Pluronic F-127 (Sigma Aldrich) were used as classic pore precursors. Nano-nonwoven were

obtained in-house using electrospinning technique with polyvinylpyrrolidone,  $M_n$  1,300,000 g/mol, Sigma Aldrich. 1,4-Dioxane, methanol, and POCh SA, were used as solvents. Ultrapure water with 18.2 M $\Omega$ cm conductivity was obtained using MiliQ device.

## 2.1 | Preparation of scaffolds

The solutions of each polymer in 50 ml of 1,4-dioxane were prepared (Table 1). The solutions were mixed by 24 hr on a magnetic stirrer (200 rpm) in room temperature. After this time, optionally one or two classic pore precursors were added to the solutions in a suitable weight ratio to dioxane (Table 1). Scaffolds were obtained by inversion phase method (Figure 1). Polyesters solution in dioxane with classic pore precursor or without them was poured onto a glass base. Polyvinylpyrrolidone ( $M_n$  10 kg mol) nano-nonwoven was placed on the solution layer after pouring, and subsequently, the air was removed by applying pressure. Next, the subsequent layer of the solution was poured, and nano-nonwoven was placed once again. At the end, the air was removed once again from the formed membrane-forming solution. The membrane was gelled in water with a conductivity of 18.2 M $\Omega$ cm. The membrane was dried after polymer coagulation and removal of pore precursors. Scaffolds without pore precursor were obtained analogically without the stage of the addition of polymeric nano-nonwoven.

## 2.2 | Mechanical strength

Scaffold mechanical strength was tested in a tensile test using an Instron 5566 apparatus. Rectangles of 7 × 2 cm cut from the scaffolds, three replicates per each scaffold, were tested. The samples were extended at a rate of 5 mm/min, and then the average values of Young's

modulus ( $E$ ), maximal strain ( $\epsilon_{max}$ ), and their standard deviation were calculated. Each experiment was done three times.

## 2.3 | Scanning electron microscopy

Morphology of cross-sections for membranes and both surfaces were analyzed using scanning electron microscopy (SEM) on Hitachi TM1000. Samples of the membranes were immersed in ethanol and then fractured in liquid nitrogen. After drying, the membrane samples were coated with 7–10 nm thick gold layer using K550X Sputter Coater. Samples coated with gold were analyzed in ×300 and ×1000 magnifications using 15 kV acceleration voltage. Average porosity and pore diameter range based were determined based on the image analysis using MeMoExplorerTM software.

## 2.4 | Isopropyl alcohol mass absorbability

Dry weighed samples were placed in a beaker with isopropyl alcohol (iPrOH) and then put for 30 min into a desiccator connected to a vacuum pump. After this time, the samples were removed from the desiccator, the excess of isopropyl alcohol was removed from them, and then, they were weighed on an analytical balance. Each experiment was done in triplicate. Absorbability was calculated according to the following Equation (1):

$$A_m = \frac{m_w - m_s}{m_s} \times 100\% \quad (1)$$

where,  $m_w$  is the mass of the wet air-weighed sample (g);  $m_s$  is the mass of the air-weighed dry sample (g); and  $A_m$  is the mass absorbability (%).

**TABLE 1** The compositions of solutions used in wet inversion phase method

Polymer	$C_{wt}$ (%)	Pore precursor	Precursor: polymer (g/g)
PLLA	6	–	–
PCL	6	–	–
PCLA	8	–	–
PLLA	6	PVP	1:1
		PVP + PEG	1:1:2
PLLA	6	PVP nano-nonwoven	1:1
PCL	6	PVP nano-nonwoven	1:1
PCLA	6	PVP nano-nonwoven	1:1
PLLA	6	PVP nano-nonwoven + PEG	1:1:2
PLLA	6	PVP nano-nonwoven + PEG + pluronic	1:1:2:1

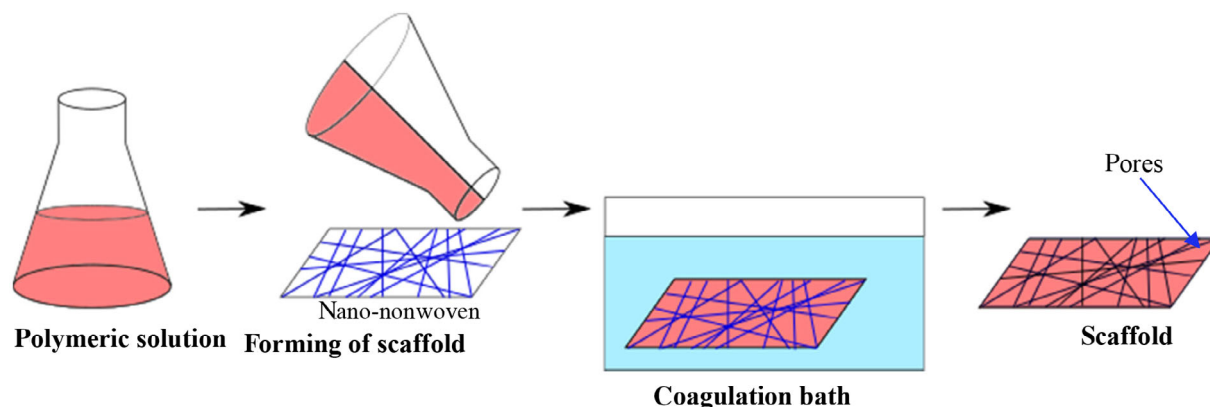


**FIGURE 1** Wet inversion phase method with polymeric nano-nonwoven [Color figure can be viewed at [wileyonlinelibrary.com](http://wileyonlinelibrary.com)]

## 2.5 | Horse plasma absorbability

A scaffold sample was placed in a flask with a capacity of 15 ml, which was filled subsequently with serum isolated from equine blood. The flask was placed in a dryer at 37°C for 24 hr or centrifuged in an Eppendorf Centrifuge 5804R laboratory centrifuge for 15 min (37°C, 5000 rpm). After this time, the sample was removed from the flask and weighed on an analytical balance. Each experiment was done in triplicate.

## 2.6 | Infrared spectroscopy

Infrared (IR) spectra of the sample were recorded by the ATR technique using an Alpha Bruker instrument. Dry samples without pre-preparation were used in the study. Each experiment was done in triplicate.

## 2.7 | Elemental analysis

Elemental composition of the samples (contents of C, H, N, and S) was examined using an Elementar Vario EL III instrument. Dry samples without prepreparation were used in the study. Analysis of every sample was done in triplicate.

## 2.8 | Cytotoxicity

The scaffolds were washed in a 0.9% NaCl solution, and then, discs with a diameter of 7.0 mm were cut from them and placed in 24-well plates. Next, Jurkat cells suspended in a nutrient medium, with a concentration of  $1 \times 10^6$  cells/ml were placed in the wells. Cell cultures in the presence of the studied samples were carried out for 11 days at 37°C, under an atmosphere of 5% CO<sub>2</sub>. In the 1st, 4th, and 8th day, the cells were analyzed in a flow cytometer, using a cytochemical reaction with propidium iodide.

## 2.9 | Chondrocyte primary culture

### 2.9.1 | Preparation of nutrient medium

About 100 ml of DMEM (with a high level of glucose and 4500 mg of L-glutamine) were dissolved in 1 L of deionized water, then 4.3% of inactivated FBS, 0.85% of the penicillin–streptomycin solution, 0.43% of L-glutamine, and 0.05% of amphotericin were added.

### 2.9.2 | Isolation of cells

Chondrocytes were isolated from human knee or iliac joint being a postsurgical waste (Bioethical Commission approval No. 57/PB/2014). Cartilaginous tissue was cut out from the joint, cut into smaller pieces using a scalpel, and washed with PBS and DMEM three times. The comminuted tissue was placed in a collagenase solution in the nutrient medium, and then heated to 37°C and filtered through a syringe filter with 0.2 μm pores. The tissue was transferred into 50-ml flasks containing a digesting solution and kept in an incubator for 16 hr. After this time, the contents of the flasks were filtered through a syringe filter with 0.7 μm pores and then centrifuged in a laboratory centrifuge (5 min, 5°C, and 1000 rpm). The obtained cellular precipitate was suspended in 10 ml of the medium and centrifuged again to remove collagenase. About 1 ml of cellular suspension was obtained.

### 2.9.3 | Preparation of samples for culturing

The scaffolds were sterilized in ethanol, and discs having a diameter of 16 mm were cut from them. Then, the scaffolds were washed with PBS and DMEM three times to remove ethanol.

## 2.9.4 | Cell culture

The scaffolds were placed in 24-well plates and chondrocytes suspended in the nutrient medium were inoculated on them. The samples were loaded down with Teflon rings. Cell culture was carried out in an incubator, at a temperature of 37°C, and under an atmosphere containing 5% CO<sub>2</sub>. The nutrient medium was replaced twice a week, then heated to 37°C. Once per 2 weeks, the cells were washed with PBS.

## 2.9.5 | Hoechst test

The nutrient medium was removed from the wells, then 500 µl of 2.5% glutaraldehyde solution was added to each of them and incubated at 5°C for 1 hr. Next, one drop of Hoechst stain and 500 µl of PBS were placed on every fixed sample. The samples were observed under an OLYMPUS IX71 fluorescence microscope.

## 2.10 | Statistical analysis

The results of the measurements were expressed as means  $\pm$  SD. Statistical significance of differences was analyzed using single-factor analysis of variance (ANOVA) for  $p < 0.05$  (MS Excel 365).

# 3 | RESULTS

## 3.1 | Chart 1: Influence of nonclassic pore precursor on the morphology of scaffolds

PVP is the most commonly used porophore in the wet phase inversion method. It provides a material characterized by the presence of numerous but closed and small pores (Figure 1). Moreover, their surfaces have too low porosity, precluding the penetration of the scaffold interior by the cells (Figure 2(a),(c)). Usually, such properties are not sufficient for conducting cell cultures, therefore, noticing numerous advantages of biodegradable polymers (controlled degradation, biocompatibility, and good mechanical properties), other methods are searched for, enabling the preparation of scaffolds with properties which allow for conducting efficient cell cultures.

While searching for methods which allow for preparing of scaffolds having an adequate morphology for tissue engineering applications and noticing the insufficient effects of conventional methods, it was decided to use unconventional methods. In previous articles, cellulosic nonwovens were used as a nonclassic pore precursor. Even though pore

morphology forming thanks to them was very favorable from cell cultures, they had a disadvantage consisting in a very long time of leaching of the nonwoven fabric (~1 month). In this reason, it was decided to use polyvinylpyrrolidone nano-nonwoven, which did not require a prolonged washing bath for its dissolution, but only an ordinary water bath.

Scaffolds from three various biodegradable polymers were obtained: polylactide, poly-ε-caprolactone, and their copolymers (Figure 3, Table 2) were obtained using a PVP nano-nonwoven.

The scaffolds obtained from PLLA with an addition of a PVP nano-nonwoven were characterized by the occurrence of sparse oval pores with a size of 1–20 µm in the bottom surface. Numerous oblong mutually connected pores with sizes in the range of 20–100 µm were evident in the fracture; additionally, smaller, approximately 1-µm pores were present in their walls. Oblong and oval pores with sizes in the range of 5–20 µm, formed as a result of nanofibrils impression, were present in the porous top surface.

The bottom surface of the PCLA scaffolds contained scarce pores with sizes of 1–15 µm. Numerous open oblong pores with sizes in the range of 10–70 µm were evident in the fracture, and in their walls, also smaller pores (1–5 µm) were present. Oblong and oval pores with sizes in the range of 1–15 µm were present in the top surface.

PCL scaffolds had scarce small pores with a size of 1–30 µm in the bottom surface. Oblong irregular pores with sizes in the range of 5–50 µm were present in the fracture, and in their walls, scarce smaller pores (~1 µm). Oblong and oval pores with sizes in the range of 5–30 µm were present in the top surface.

It was found that addition of nano-nonwoven changed the morphology of the scaffolds very favorably. Unlike the scaffolds obtained with an addition of classic precursors, they were characterized by large open pores and a strongly porous top surface. Such a structure creates the possibility of conducting cell cultures. It was found that the scaffolds obtained from polylactide exhibited the most favorable structure. In comparison to the scaffolds obtained from the other polymers, were characterized by the largest pores occurring in the fracture. Therefore, they were selected for further studies.

## 3.2 | Chart 2: Influence of nonclassic and classic pore precursor on the morphology of scaffolds

We observed the favorable impact of nonclassic pore precursors on the scaffold morphology. It was decided to study the morphology of the scaffolds forming as a result of the application of both a polymer nano-nonwoven

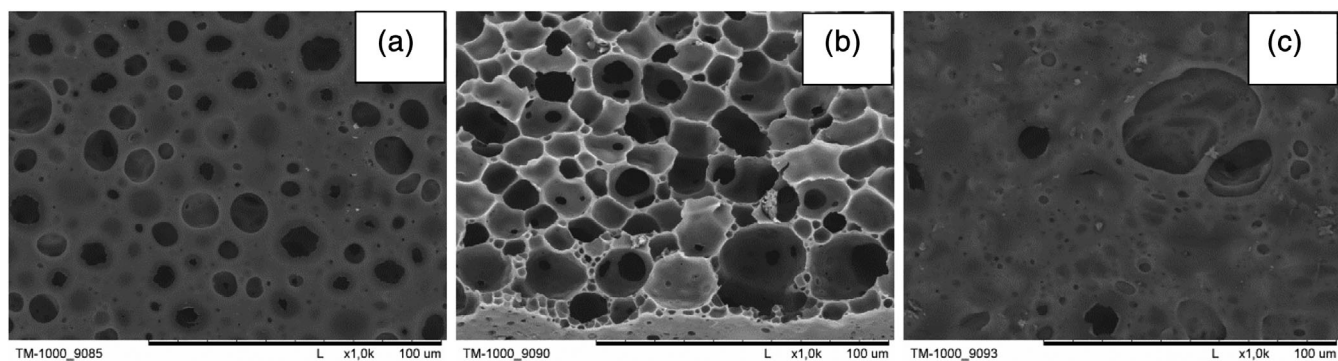


**FIGURE 2** PLLA scaffolds obtained with the addition of classic pore precursor (PVP); (a) lower surface, (b) cross-section, and (c) upper surface

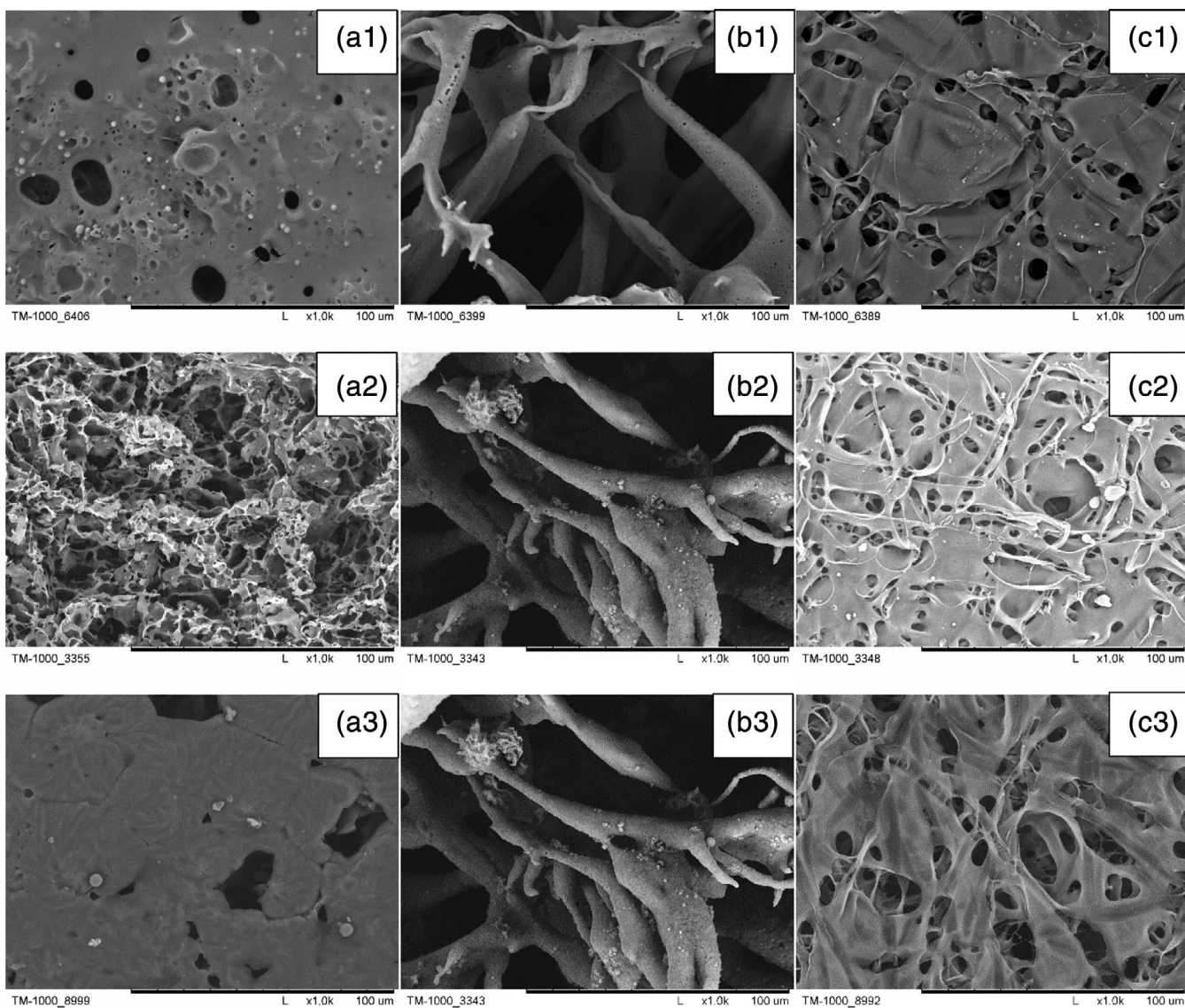


**FIGURE 3** Scaffolds obtained with the addition of PVP nano-nonwoven; (1) PLLA, (2) PCL, and (3) PCLA; (a) lower surface, (b) cross-section, and (c) upper surface

additive and a classic pore precursor [polyethylene glycol (PEG), as well as PEG and Pluronic] (Figure 4, Table 3).

In the scaffolds obtained from PLLA with an addition of a PVP nano-nonwoven and polyethylene glycol, the

**TABLE 2** Pores size of polyesters scaffolds obtained by inversion phase method using PVP nano-nonwoven

Range of pores diameter ( $\mu\text{m}$ )		
Lower surface	Cross-section	Upper surface
PLLA + PVP nano-nonwoven		
1–20	20–100, $i \sim 1$	5–20
PCLA + PVP nano-nonwoven		
1–15	10–70, $i \sim 1$ –5	1–15
PCL + PVP nano-nonwoven		
1–30	5–50, $i \sim 1$	5–30

bottom surface contained scarce pores with size in the range of 1–20  $\mu\text{m}$ . Oblong open pores with sizes in the range of 20–80  $\mu\text{m}$ , having smaller pores (1–5  $\mu\text{m}$ ) in their walls, were observed in the porous material. Numerous oblong pores with sizes in the range of 5–60  $\mu\text{m}$  were present in the top surface.

The bottom surface of the scaffolds obtained from PLLA with an addition of a PVP nano-nonwoven and a PEG–Pluronic mixture contained scarce pores with sizes in the range of 1–20  $\mu\text{m}$ . Irregular open pores with size in the range of 10–70  $\mu\text{m}$  and porous internal structure (1–10  $\mu\text{m}$ ) were present in the fracture. The top surface was characterized by the presence of numerous irregular pores with sizes in the range of 5–60  $\mu\text{m}$ .

It was found that the addition of classic pore precursors together with a polymer nano-nonwoven is favorable

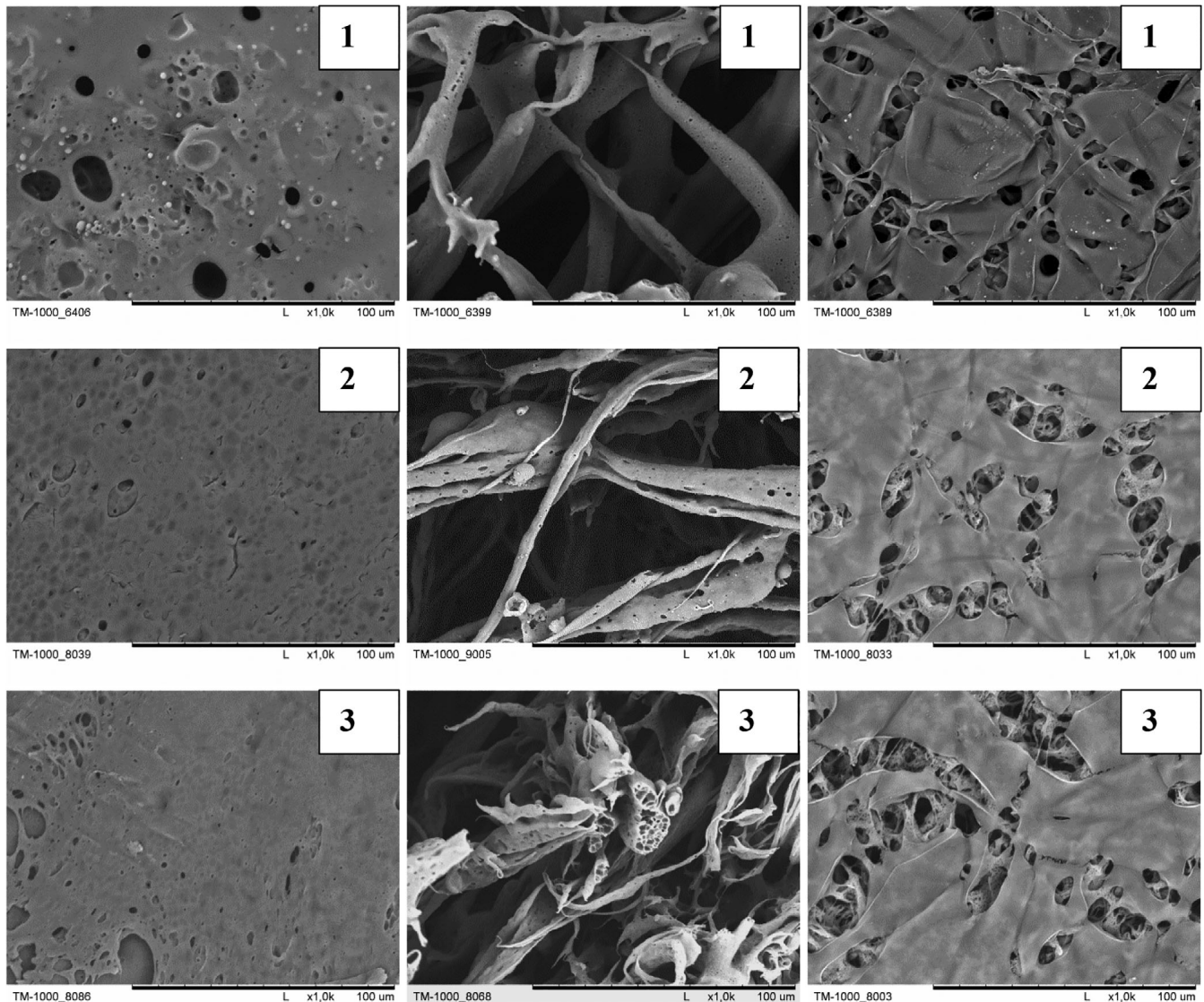


**FIGURE 4** Scaffolds obtained with the addition of PVP nano-nonwoven and classic pore precursor; (1) without classic pore precursor, (2) with PEG, and (3) with PEG and pluronic; (a) lower surface, (b) cross-section, and (c) upper surface

because it induces perforation and formation of pores occurring inside walls of the largest pores. It increases the total porosity of the scaffold, thereby facilitating the migration of nutrients and metabolites inside the scaffold.

### 3.3 | Chart 3: Mechanical properties

Adequate mechanical strength is a very important feature from the point of view of tissue engineering because the strength must match that of the tissue being regenerated. In the case of cartilaginous tissue, Young modulus must be higher than 10 MPa. Mechanical strength of the studied samples was examined in a static tensile test. Young modulus, maximum stress, and maximum strain were determined (Figure 5, Table 4). The scaffolds have a stress curve characteristic for elastic materials without material yield strength.

In the PLLA scaffolds obtained with an addition of a PVP nano-nonwoven, Young modulus amounted to  $163.1 \pm 53.7$  MPa, maximum stress  $4.87 \pm 0.95$  MPa, and maximum strain  $31.00 \pm 2.8\%$ . It was found that the studied scaffolds exhibited good mechanical properties, enabling their application in the regeneration of cartilaginous tissue because its value of Young modulus was higher than that of the tissue itself ( $E > 10$  MPa).

### 3.4 | Chart 4: Absorbability of the scaffolds

Absorbability of materials for medical applications with hydrophilic substances is a crucial element enabling migration of nutrients and body fluids. Absorbability of the scaffolds with a reference substance (isopropyl alcohol) and with horse plasma isolated from equine blood was tested (Figure 6). The latter tested substance was introduced to the scaffold by a static test and a laboratory

centrifuge test. To better show the changes in absorbability occurring after application of a polymer nano-nonwoven, the results were compared with the scaffolds obtained with an addition of only classic pore precursors.

The scaffolds obtained by wet inversion phase with a polymer nano-nonwoven exhibited much higher absorbability both with isopropyl alcohol, and equine serum [ $545.2 \pm 92.6\%$ ,  $779.4 \pm 61.6\%$  (static test), and  $843.8 \pm 162.6\%$  (centrifuge test), respectively] than the scaffolds obtained with an addition of classic pore precursors [iPrOH:  $315.7 \pm 7.2\%$ , serum:  $258.2 \pm 64.3\%$  (static test) and  $242.6 \pm 38.0\%$  (centrifuge test)]. Also, it was proved that the differences in absorbability obtained by the static test are small.

It was found that the studied scaffolds, although were composed of polymers with hydrophobic properties, absorbed hydrophilic substances very well due to their unique structure.<sup>28</sup> It is a necessary condition for their subsequent application in tissue engineering.

### 3.5 | Chart 5: Nano-nonwoven residues

Composition of products intended for medical applications is a very important element. Because the applied polymeric nano-nonwoven was being leached from the scaffold structure, it was decided to examine presence (IR analysis) (Figure 7) and content (elemental analysis) (Table 5) of its residue in the obtained scaffolds. The test was carried out based on an analysis of polylactide and PVP nano-nonwoven in scaffold before and after a washing bath.

In IR spectra of the scaffolds before the washing bath, presence of PVP (band in the range of  $3600\text{--}3000\text{ cm}^{-1}$ ) and PLLA (bands at  $1750$  and  $1180\text{ cm}^{-1}$ ) (Figure 7, red line) is clearly visible. In the spectra of dried scaffolds

**TABLE 3** Porosity analysis of PLLA scaffolds obtained with the addition of PVP nano-nonwoven and classic pore precursors

Range of pores diameter ( $\mu\text{m}$ )		
Lower surface	Cross-section	Upper surface
PLLA + PVP nano-nonwoven		
1–20	20–100/~1	5–20
PLLA + PVP nano-nonwoven + PEG		
1–20	20–80/1–5	5–60
PLLA + PVP nano-nonwoven + PEG + pluronic		
1–20	10–70/1–10	5–60

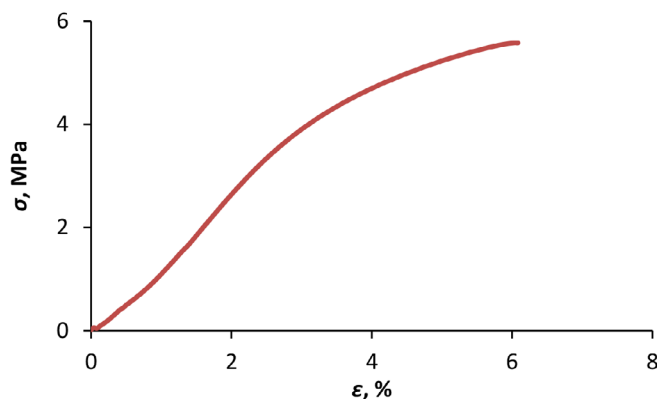


**FIGURE 5** Exemplary stress–strain curve of PLLA scaffolds obtained with the addition of PVP nano-nonwoven [Color figure can be viewed at [wileyonlinelibrary.com](http://wileyonlinelibrary.com)]

after gelling and washing baths (Figure 7, green line), only bands originating from PLLA are evident.

To determine the quantitative content of the PVP nano-nonwoven in the obtained scaffolds, elemental analysis of the samples was carried out. The nano-nonwoven itself was characterized by a high nitrogen content (10.41%). Analogically, a significant nitrogen content (8.24%) was found before the washing bath in the scaffolds obtained with an addition of nano-nonwovens. On the other hand, the nitrogen content was below the

limit of determination after the washing bath. It proves complete leaching of the nano-nonwovens from the structure of the scaffolds or the fact that only their traces remained.

### 3.6 | In vitro studies

#### 3.6.1 | Cytotoxicity

Cytotoxicity of the scaffolds obtained by the wet inversion phase method using a PVP nano-nonwoven was determined using T lymphocytes. The cultures were conducted in a contact test, examining the top surface (onto which the nano-nonwoven was placed) (Figure 8).

After 24 hr of lymphocyte culturing, their number decreased slightly in relation to the control ( $97 \pm 0.7\%$ ) and amounted to  $96 \pm 0.5\%$ . After 96 hr of culture, the number of cells in the scaffold increased ( $98 \pm 0.2\%$ ). After 192 hr, the number of cells in scaffolds from PVP nano-nonwoven decreased slightly ( $94 \pm 0.6\%$ ).

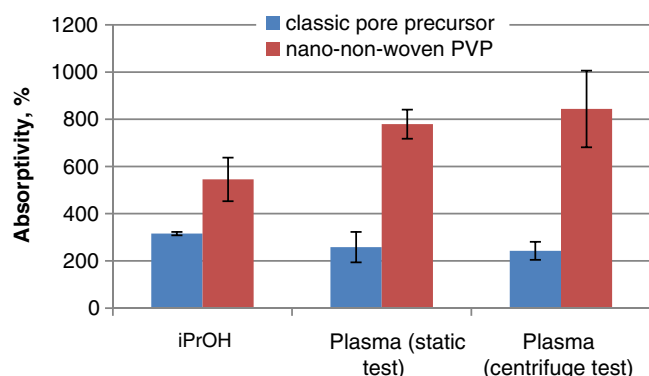
#### 3.6.2 | Chondrocyte culture

Various inoculation densities of human chondrocyte cells were examined:  $1 \times 10^5$ ,  $2 \times 10^5$ , and  $2.5 \times 10^5$  of cells per well. Then, after 72 hr of culture, the cells in the scaffolds were stained in the Hoechst test (Figure 9).

At the inoculation density of  $1 \times 10^5$ , only small cellular aggregates were visible. The  $2 \times 10^5$  suspensions, a higher number of cells was obtained, the majority of them being agglomerated. At the density of  $2.5 \times 10^5$ , the

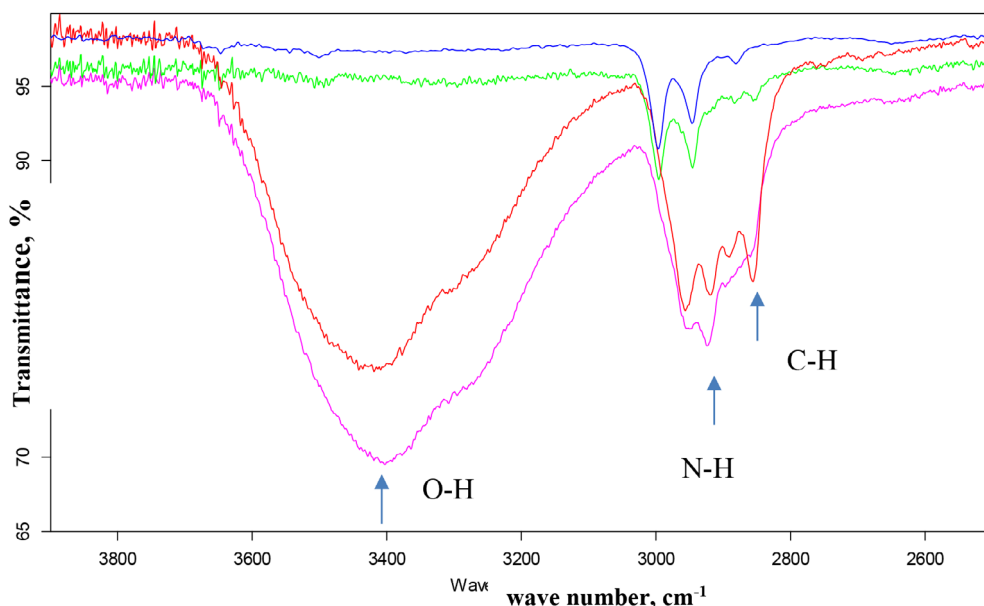
**TABLE 4** Mechanical properties of scaffolds obtained by inversion phase method using PVP nano-nonwoven

<i>E</i> (MPa)	$\sigma$ (MPa)	$\epsilon$ (%)
$163.1 \pm 53.7$	$4.87 \pm 0.95$	$31.00 \pm 2.8$



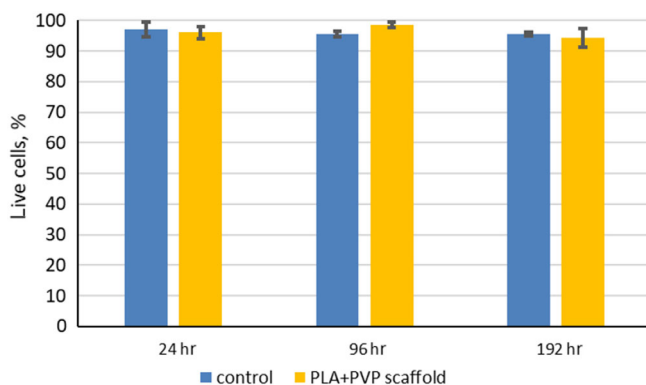
**FIGURE 6** Absorptivity of scaffolds obtained with addition nonclassic pore precursor and with nano-nonwoven [Color figure can be viewed at [wileyonlinelibrary.com](#)]

**FIGURE 7** IR analysis: Blue line—PLLA, violet line—PVP nano-nonwoven, red line—PLLA scaffolds with PVP nano-nonwoven before coagulation bath, and green line—PLLA scaffolds with PVP nano-nonwoven after coagulation bath [Color figure can be viewed at [wileyonlinelibrary.com](#)]



**TABLE 5** Content of elements in scaffolds obtained with PVP nano-nonwoven

Sample	Content of elements (%)		
	C	H	N
PLLA	49.87	5.62	–
PVP nano-nonwoven	54.47	8.66	10.41
Scaffold before rinsing bath	54.33	8.66	8.24
Scaffold after rinsing bath	50.08	5.16	–

**FIGURE 8** The changes in the number of viable T lymphocytes cells in time (blue bars—control, yellow bars—PLA scaffold obtaining with PVP nano-nonwoven, and red line—limit of cytotoxic effect) [Color figure can be viewed at [wileyonlinelibrary.com](http://wileyonlinelibrary.com)]

number of the cells was highest, and they were scattered. It was considered that the cell density of  $1 \times 10^5$  is too low to form an efficient chondrocyte culture. For the sake of a relatively small amount of cartilaginous tissue in available medical waste, constituting the chondrocyte source, it was decided to use cell density equal to  $2 \times 10^5$ .

### 3.6.3 | Chondrocyte culture on scaffolds

A chondrocyte culture with a cell density of  $2 \times 10^5$ /well was conducted. Samples were collected from the culture (after 3 days, 1 week, 2 weeks, and 3.5 weeks) and analyzed. The exposed cells grown in the scaffolds were stained by Hoechst test (Figure 10).

After 3 days, the presence of chondrocytes was observed in the scaffolds, mainly agglomerated in aggregates. After 1 week, the number of cells increased, and they underwent scattering, indicating the fact they began to relocate into pores of the scaffold. After 2 weeks, the number of cells and their location did not change significantly. On the other hand, after 3.5 weeks, the cells underwent a repeated scattering, but their number—

considering their scattering—did not change significantly. Moreover, it was observed that the stain (Hoechst) was distributed irregularly in nuclei of the cells (stain scattering), which could indicate damage to the chondrocytes.

### 3.6.4 | Morphology of the tissue in the scaffolds

SEM analysis of properly prepared and dried samples of the scaffolds with cells was carried out (Figure 11).

After 3 days, practically no tissue was observed in SEM images. After 1 week, protein forming between the pores and cell nuclei started to be observed. After 2 weeks, a slight increase in the amount of protein and the number of cell nuclei were evident. Moreover, impurities adhering to the cells were observed. After 3.5 weeks, a distinctly larger amount of protein covering the polylactide surface was observed. Under high magnification ( $\times 3000$ ), PLLA may be distinguished from protein, which, unlike the polymer, did not melt.

The scaffolds obtained using a PVP nano-nonwoven do not exhibit a cytotoxic impact on T lymphocytes (number of cells  $\gg 70\%$  of their initial number), which allows for ascertaining that these scaffolds may be used for culturing other cells.

## 4 | DISCUSSION

The wet inversion phase method gives cell scaffolds to high porosity (above 80%). Unfortunately, the pores obtained are small (10–50 microns).<sup>25</sup> The most common epidermal layer is presented in these scaffolds.<sup>50</sup> It makes it difficult for cells to access the pores inside the scaffolds. Cells cannot grow properly.<sup>52</sup> They do not form a 3D structure that is necessary for the reconstruction of cartilage. Cells grow flat on scaffoldings obtained by classical methods. They often do not produce adequate protein structures necessary for proper differentiation. The modification introduced by us allows obtaining much larger pores (up to 100 microns). Scaffoldings are characterized by a much higher overall porosity of approximately High regularity in the internal structure is observed, which contributes to obtaining homogeneous tissue cultures. In the scaffoldings we receive, there is no epidermal layer that closes access to the inside of the scaffold. This is especially beneficial, especially in cartilage regeneration. Cartilage can grow in three dimensions, which is necessary for its proper functioning. The

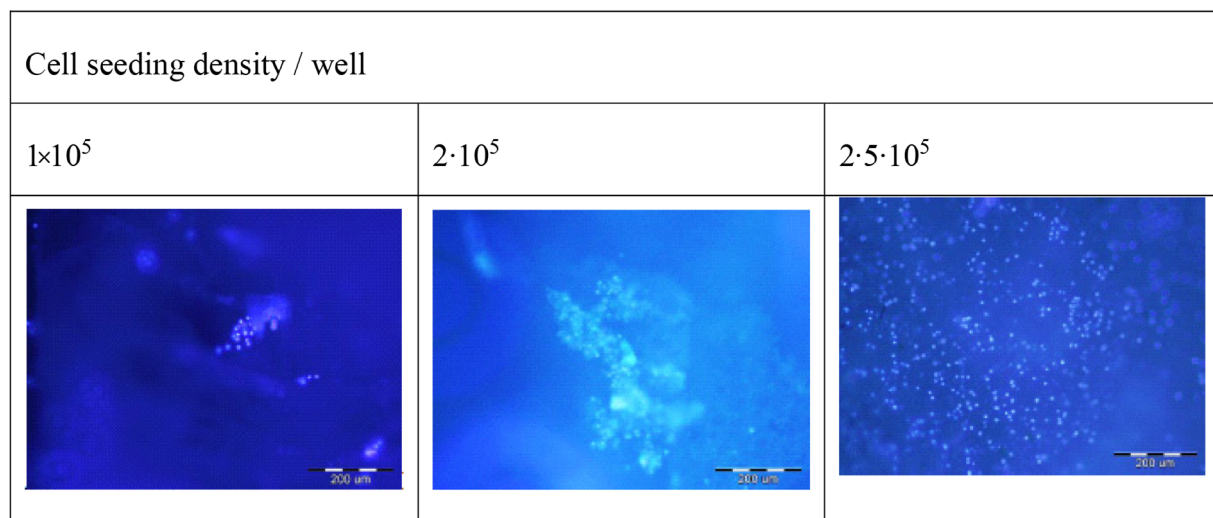


**FIGURE 9** Images of scaffolds with different seeding densities, with Hoechst stained cells after 72 hr of culture ( $\times 10$  magnification) [Color figure can be viewed at [wileyonlinelibrary.com](http://wileyonlinelibrary.com)]

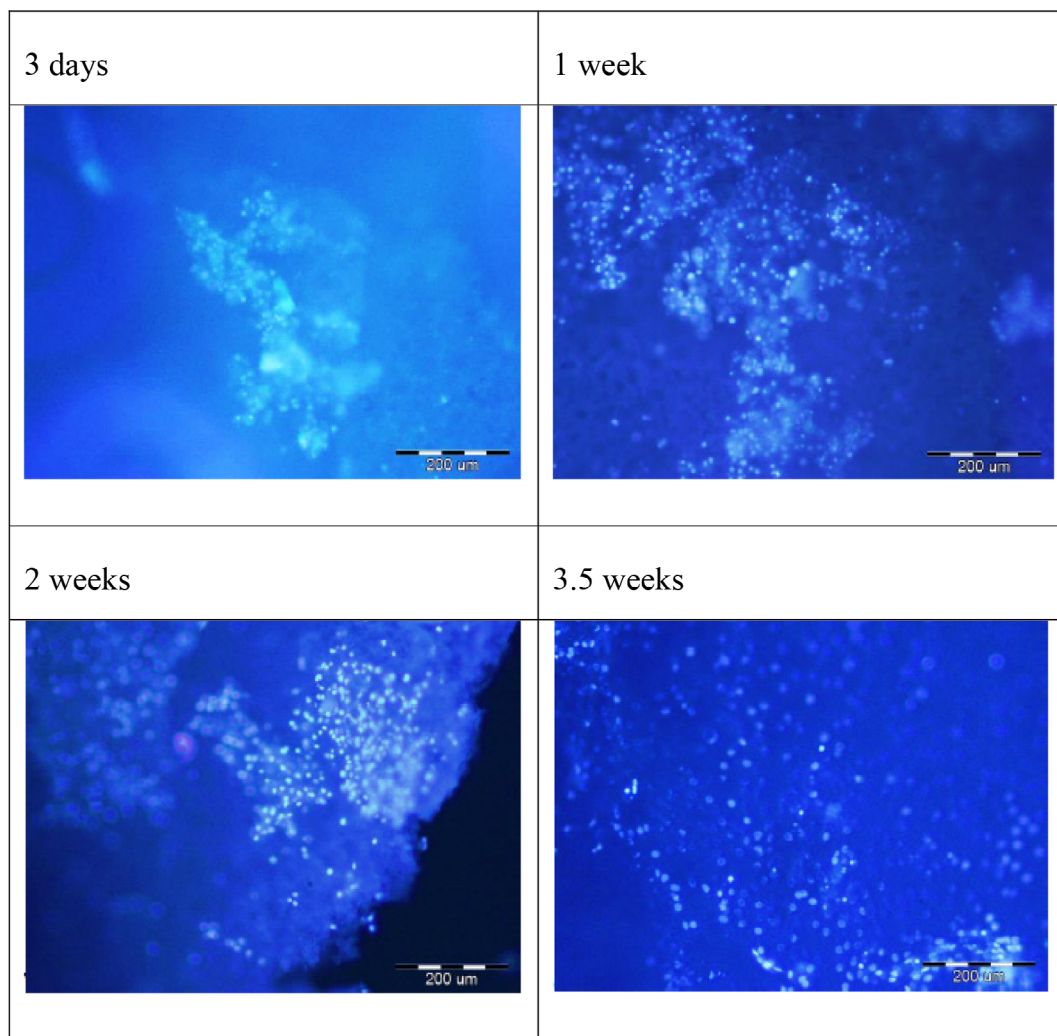


**FIGURE 10** Images of scaffolds with stained Hoechst cells after 3 days and 1, 2, and 3.5 weeks of culture ( $\times 10$  magnification) [Color figure can be viewed at [wileyonlinelibrary.com](http://wileyonlinelibrary.com)]

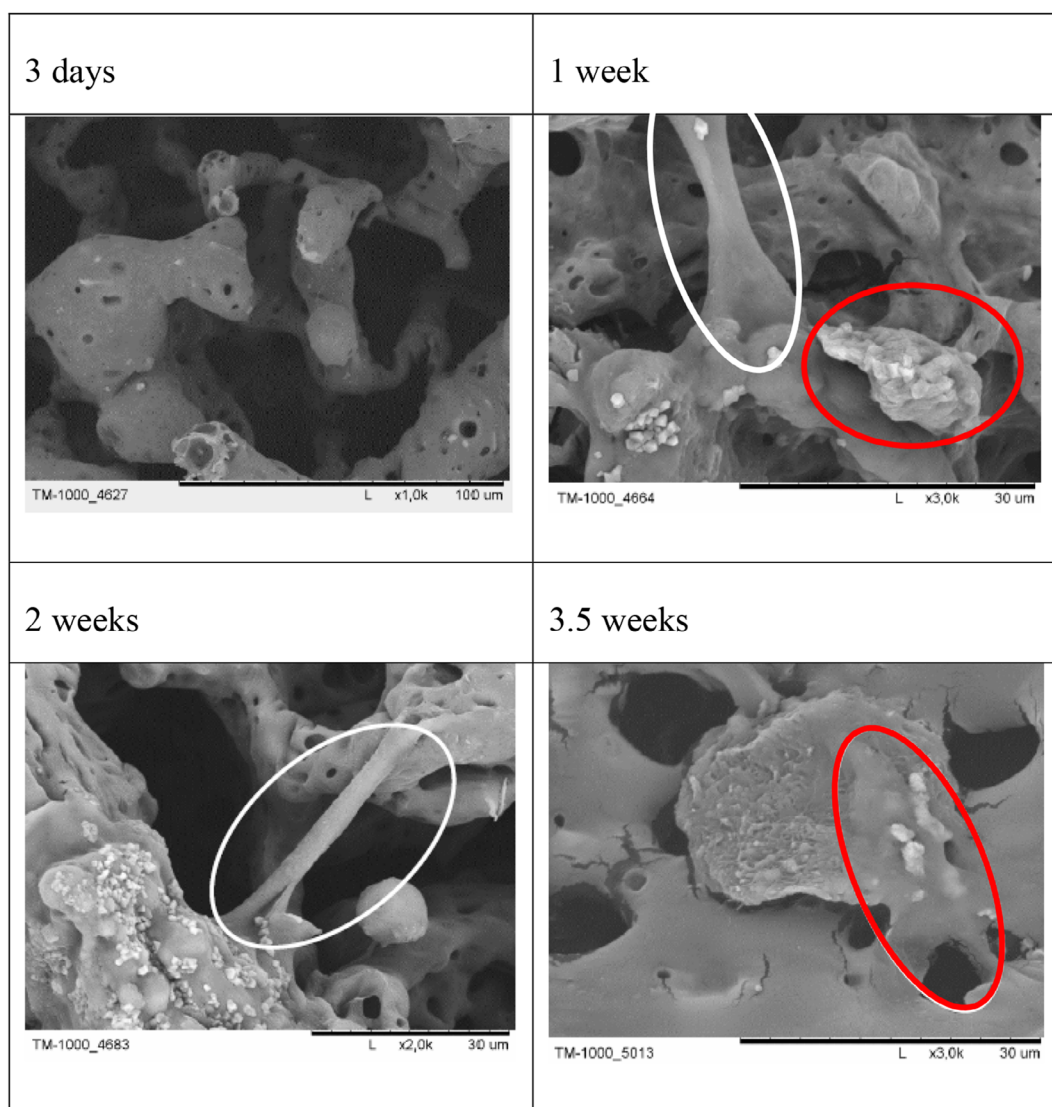


**FIGURE 11** SEM images of scaffolds after 3 days, 1, 2, and 3.5 weeks of cell culture on scaffolds (enlargements selected to best visualize the resulting structures); cells are marked with the red circle, protein fibers with the white circle [Color figure can be viewed at [wileyonlinelibrary.com](http://wileyonlinelibrary.com)]

morphology on the scaffolding surface is very similar to that occurring inside. In addition, there are micro-perforations in the pores that facilitate the introduction of nutrients and the removal of cellular metabolites.<sup>35</sup>

The use of PVP nano-nonwoven as a porogen brought a double benefit. First of all, you can easily influence the shape and arrangement of pores. Internal morphology is like an imprint of the morphology and arrangement of fibers in a nonwoven fabric. The regularity of the pores obtained is reproduced with an accuracy similar to that obtained using 3D printing.<sup>49</sup> The advantage of our solution compared with 3D printing is a lower process temperature. This positively affects the mechanical properties of the scaffold. The following processes are

limited, for example, depolymerization, which may occur in polyesters under the influence of temperatures above 150°C. So the medical product is also chemical cleaner.

The second advantage of using PVP nano-nonwoven is not apparent. It is generally believed that polylactide scaffolds are highly hydrophobic. Therefore, they are not suitable for settling cells on them. The authors of earlier works believe that it is difficult to inject a suspension of culture medium into the scaffolding precisely because of this hydrophobicity.<sup>15</sup> In our process, some PVP remains on the surface of the pores. As a result, it hydrolyzes the surface inside the scaffolding. Thanks to that the absorbability with hydrophilic media is definitely higher than in scaffoldings obtained by the classical variants of the

inversion phase method.<sup>19</sup> The positive effect of amino groups on cell development is well known. In scaffolds obtained using PVP, there are enough of them to improve the absorbability of the scaffolding and positively affect cell development.

Many studies have previously shown that an increase in scaffold porosity significantly weakens mechanical properties.<sup>21</sup> The scaffolds which we received had similar properties. We observed a decrease in breaking strength. However, the flexibility of the scaffolds expressed as Young's modulus increased. Greater flexibility while maintaining elasticity is very beneficial from the point of application of the scaffold. It should be easier to insert such an implant endoscopically, which reduces the risk of complications for the patient.<sup>6</sup>

We have shown that adequate morphology and hydrolysis of common pores in the scaffold is nontoxic to T lymphocytes and cartilage cells are taken from the patients. Microscopic observations confirmed the usefulness of the developed scaffolds in cell cultures, especially cartilage. We were the first to show the results of long-term breeding of chondrocytes on scaffolds (about 4 weeks). Earlier work mainly described short-term cultures aimed at assessing scaffold toxicity to cells.<sup>18</sup> We have shown that the cells do not grow individually as previously reported. In our case, they grow whole colonies and produce protein structures. This indicates a favorable ground for chondrocytes proliferation and growth.

## 5 | CONCLUSION

Addition of polymer nano-nonwovens is very favorable. The pores are large, open, and contain numerous perforations of their side walls. Simultaneous application of classic pore precursors together with a polymeric nano-nonwoven leads to an increase in the perforation of side walls of large pores, creating the possibility of better intercellular communication and migration of nutrients and metabolites. Despite a high porosity of the fracture, the obtained scaffolds, maintain very good mechanical properties, and sufficient for the regeneration of cartilaginous tissue. Even though the obtained scaffolds are composed of polymers with hydrophobic character, they exhibit very good hydrophilic properties, which results indirectly from presence of micropores in their structure. The PVP nano-nonwoven used in the process of scaffold preparation is being practically completely removed from the scaffold structure by washing out. The cellular studies carried out using T lymphocytes proved a lack of toxicity of the scaffolds toward the cells unambiguously. In tests using

chondrocyte cell collected from patients, a uniform distribution of the cells on the surface of the scaffold and in its interior was observed. It proves an adequate scaffold morphology and good adhesion of the cells to the substrate.

## ACKNOWLEDGMENT

This study was financially supported by the Warsaw University of Technology.

## CONFLICT OF INTEREST

The authors declare no conflicts of interest.

## ORCID

Agnieszka Gadomska-Gajadhur  <https://orcid.org/0000-0001-7686-1745>

## REFERENCES

- [1] F. Flaig, H. Ragot, A. Simon, G. Revet, M. Kitsara, L. Kitasato, A. Hébraud, O. Agbulut, G. Schlatter, *ACS Biomater. Sci. Eng.* **2020**, 6, 2388.
- [2] R. Langer, J. P. Vacanti, C. A. Vacanti, A. Atala, L. E. Freed, G. Vunjak-Novakovic, *Tissue Eng.* **1995**, 1, 151.
- [3] M. Mhaske, P. Kedar, S. Bansode, *Int. J. Adv. Res. Dev.* **2017**, 2, 280.
- [4] F. J. O'Brien, *Mater. Today* **2011**, 14, 88.
- [5] C. M. Murphy, F. J. O'Brien, D. G. Little, A. Schindeler, *Eur. Cell Mater.* **2013**, 26, 120.
- [6] S. Rhee, J. L. Puetzer, B. N. Mason, C. A. Reinhart-King, L. J. Bonassar, *ACS Biomater. Sci. Eng.* **2016**, 2, 1800.
- [7] Q. L. Loh, C. Choong, *Tissue Eng. Part B Rev.* **2013**, 19, 485.
- [8] T. Garg, O. Singh, S. Arora, R. S. R. Murthy, *Crit. Rev. Ther. Drug Carr. Syst.* **2012**, 29, 1.
- [9] M. I. Baker, S. P. Walsh, Z. Schwartz, B. D. Boyan, *J. Biomed. Mater. Res. Part B: Appl. Biomater.* **2012**, 100, 1451.
- [10] H. Fernandes, L. Moroni, C. van Blitterswijk, J. de Boer, *J. Mater. Chem.* **2009**, 19, 5474.
- [11] C. Frantz, K. M. Stewart, V. M. Weaver, *J. Cell Sci.* **2010**, 123, 4195.
- [12] A. D. Theocharis, S. S. Skandalis, C. Gialeli, N. K. Karamanos, *Adv. Drug Deliv. Rev.* **2016**, 97, 4.
- [13] H. Geckil, F. Xu, X. Zhang, S. Moon, U. Demirci, *Nanomedicine* **2010**, 5, 469.
- [14] Y. Kim, H. Ko, I. K. Kwon, K. Shin, *Int. Neurorol. J.* **2016**, 20, 23S23.
- [15] C. Insomphun, J.-A. Chuah, S. Kobayashi, T. Fujiki, K. Numata, *ACS Biomater. Sci. Eng.* **2017**, 3, 3064.
- [16] B. Mollon, R. Kandel, J. Chahal, J. Theodoropoulos, *Osteoarthr. Cartil.* **2013**, 21, 1824.
- [17] K. Mithoefer, R. J. Williams 3rd., R. F. Warren, H. G. Potter, C. R. Spock, E. C. Jones, T. L. Wickiewicz, R. G. Marx, *J. Bone Joint Surg. Am.* **2005**, 87, 1911.
- [18] P. Niemeier, D. Albrecht, S. Andereya, P. Angele, A. Ateschrang, M. Aurich, M. Baumann, U. Bosch, C. Erggelet, S. Fickert, H. Gebhard, K. Gelse, D. Günther, A. Hoburg, P. Kasten, T. Kolombe, H. Madry, S. Marlovits, N. M. Meenen, P. E. Müller, U. Nöth, J. P. Petersen, M. Pietschmann, W.

- Richter, B. Rolauffs, K. Rhunau, B. Schewe, A. Steinert, M. R. Steinwachs, G. H. Welsch, W. Zinser, J. Fritz, *Knee* **2016**, 23, 426.
- [19] J. Buckwalter, H. Mankin, *Arthritis Rheum.* **1998**, 41, 1331.
- [20] C. Erggelet, P. Vavken, *J. Clin. Orthop. Trauma* **2016**, 7, 145.
- [21] J. D. Harris, R. A. Siston, P. X. RA, D. C. Flanigan, *J. Bone Joint Surg.* **2010**, 92, 2220.
- [22] P. H. Chao, S. Yodmuang, X. Wang, L. Sun, D. L. Kaplan, G. Vunjak-Novakovic, *J. Biomed. Mater. Res. Part B: Appl. Biomater.* **2010**, 95, 84.
- [23] Y. Jiang, Y. Cai, W. Zhang, Z. Yin, C. Hu, T. Tong, P. Lu, S. Zhang, D. Neculai, R. S. Tuan, H. W. Ouyang, *Stem Cells Transl. Med.* **2016**, 5, 733.
- [24] Y.-C. Chen, R. N. Chen, H. J. Jhan, D. Z. Liu, H. O. Ho, Y. Mao, J. Kohn, M. T. Sheu, *Tissue Eng. Part C Methods* **2015**, 21, 971.
- [25] E. Popa, R. Reis, M. Gomes, *Biotechnol. Appl. Biochem.* **2012**, 59, 132.
- [26] J. Wasiak, C. Clar, E. Villanueva, *Cochrane Database of Syst. Rev.* **2006**, 3, 1465.
- [27] H. J. Chung, T. G. Park, *Adv. Drug Deliv. Rev.* **2007**, 59, 249.
- [28] A. J. T. Teo, A. Mishra, I. Park, Y.-J. Kim, W.-T. Park, Y.-J. Yong-Jin Yoon, *ACS Biomater. Sci. Eng.* **2016**, 2, 454.
- [29] L. Richert, P. Lavalle, D. Vautier, B. Senger, J. F. Stoltz, P. Schaaf, J. C. Voegel, C. Picart, *Biomacromolecules* **2002**, 3, 1170.
- [30] N. Goonoo, A. Bhaw-Luximon, G. L. Bowlin, D. Jhurry, *Polym. Int.* **2013**, 62, 523.
- [31] U. Stachewicz, T. Qiao, S. C. Rawlinson, F. V. Almeida, W. Q. Li, M. Cattell, A. H. Barber, *Acta Biomater.* **2015**, 27, 88.
- [32] V. L. Chavez, L. Song, S. Barua, X. Li, Q. Wu, D. Zhao, K. Rege, B. D. Vogt, *Acta Biomater.* **2010**, 6, 3035.
- [33] O. Jeznach, D. Kołbuk, P. Sajkiewicz, *J. Biomed. Mater. Res. Part A* **2018**, 106, 2762.
- [34] D. W. Hutmacher, *Biomaterials* **2000**, 21, 2529.
- [35] A. J. Steward, Y. Liu, D. R. Wagner, *Biomater. Reg. Med.* **2011**, 63, 74.
- [36] F. T. Zohora, A. Y. M. A. Azim, *Eur. Sci. J.* **2014**, 10, 186.
- [37] S. Liao, C. K. Chan, S. Ramakrishna, *Mater. Sci. Eng. C* **2008**, 28, 1189.
- [38] B. S. Kim, I. K. Park, T. Hoshiba, H. L. Jiang, Y. J. Choi, T. Akaike, C. S. Chong-Su Cho, *Prog. Polym. Sci.* **2011**, 36, 238.
- [39] S. Caddeo, M. Boffito, S. Sartori, *Front. Bioeng. Biotechnol.* **2017**, 5, 40.
- [40] A. Kruk, A. Gadomska-Gajadthur, P. Ruśkowski, A. Chwojnowski, J. Dulnik, L. Synoradzki, *Desalin. Water Treat.* **2017**, 64, 317.
- [41] P. Denis, M. Wrzeczionek, A. Gadomska-Gajadthur, P. Sajkiewicz, *Polymer* **2019**, 11, 2113.
- [42] R. Tuli, W. J. Li, R. S. Tuan, *Arthritis Res. Ther.* **2003**, 5, 235.
- [43] H. A. Leddy, H. A. Awad, F. Guilak, *J. Biomed. Mater. Res. Part B: Appl. Biomater.* **2004**, 70, 397.
- [44] C. J. Bettinger, *Macromol. Biosci.* **2011**, 11, 467.
- [45] A. Cheng, Z. Schwartz, A. Kahn, X. Li, Z. Shao, M. Sun, Y. Ao, B. D. Boyan, H. Chen, *Tissue Eng. Part B: Rev.* **2019**, 25, 14.
- [46] H. Y. Cheung, K. T. Lau, T. P. Lu, D. Hui, *Composites Part B: Eng.* **2007**, 38, 291.
- [47] C. Wang, N. Feng, F. Chang, J. Wang, B. Yuan, Y. Cheng, H. Liu, J. Yu, J. Zou, J. Ding, X. Chen, *Adv. Healthcare Mater.* **2019**, 8, 1900312.
- [48] Y. S. Lai, W. C. Chen, C. H. Huang, C. K. Cheng, K. K. Chan, T. K. Chang, *PLoS One* **2015**, 10, e0127293.
- [49] Y. Du, X. Chen, Y. Hag Koh, B. Lei, *Mater. Lett.* **2014**, 122, 62.
- [50] C. J. Little, N. K. Bawolin, X. Chen, *Tissue Eng. Part B: Rev.* **2011**, 17, 213.
- [51] A. H. Reddi, J. Becerra, J. A. Andrades, *Tissue Eng. Part B: Rev.* **2011**, 17, 301.
- [52] A. S. Hoffman, *Adv. Drug Deliv. Rev.* **2002**, 54, 18.
- [53] C. R. Chu, M. Szczodry, S. Bruno, *Tissue Eng. Part B: Rev.* **2010**, 16, 105.
- [54] M. W. Wong, L. Qin, J. K. Tai, S. K. Lee, K. S. Leung, K. M. Chan, *J. Biomed. Mater. Res. Part B: Appl. Biomater.* **2004**, 70, 362.
- [55] S. H. Hsu, H. J. Yen, C. S. Tseng, C. S. Cheng, C. L. Tsai, *J. Biomed. Mater. Res. Part B: Appl. Biomater.* **2007**, 80, 519.
- [56] A. Kruk, A. Gadomska-Gajadthur, I. Rykaczewska, J. Dulnik, P. Ruśkowski, L. Synoradzki, *J. Biomed. Mater. Res. Part B: Appl. Biomater.* **2019**, 107, 1079.
- [57] A. Gadomska-Gajadthur, M. Wrzeczionek, G. Matyszczyk, P. Piętowski, M. Więclaw, P. Ruśkowski, *Org. Process Res. Dev.* **2018**, 22, 1793.
- [58] S. Ramakrishna, J. Mayer, E. Wintermantel, K. W. Leong, *Compos. Sci. Technol.* **2001**, 61, 1189.
- [59] A. Chwojnowski, K. Dudziński, C. Wojciechowski, E. Łukowska, *J. Membr. Sci.* **2008**, 313, 296.
- [60] M. Guvendiren, J. Molde, R. M. D. Soares, J. Kohn, *ACS Biomater. Sci. Eng.* **2016**, 2, 1679.

**How to cite this article:** Gadomska-Gajadthur A, Kruk A, Dulnik J, Chwojnowski A. New polyester biodegradable scaffolds for chondrocyte culturing: Preparation, properties, and biological activity. *J Appl Polym Sci.* 2020;e50089. <https://doi.org/10.1002/app.50089>